Available online at www.sciencedirect.com

SCIENCE DIRECT®

Spectrochimica Acta Part A 60 (2004) 3141–3154

SPECTROCHIMICA ACTA PART A

www.elsevier.com/locate/saa

Synthesis, investigation and spectroscopic characterization of piroxicam ternary complexes of Fe(II), Fe(III), Co(II), Ni(II), Cu(II) and Zn(II) with glycine and DL-phenylalanine

Gehad G. Mohamed*, Nadia E.A. El-Gamel

Chemistry Department, Faculty of Science, Cairo University, Giza, Egypt

Received 22 December 2003; accepted 27 January 2004

Abstract

The ternary piroxicam (Pir; 4-hydroxy-2-methyl-*N*-(2-pyridyl)-2H-1,2-benzothiazine-3-carboxamide 1,1-dioxide) complexes of Fe(II), Fe(III), Co(II), Ni(II), Cu(II) and Zn(II) with various amino acids (AA) such as glycine (Gly) or DL-phenylalanine (PhA) were prepared and characterized by elemental analyses, molar conductance, IR, UV-Vis, magnetic moment, diffuse reflectance and X-ray powder diffraction. The UV-Vis spectra of Pir and the effect of metal chelation on the different interligand transitions are discussed in detailed manner. IR and UV-Vis spectra confirm that Pir behaves as a neutral bidentate ligand coordinated to the metal ions via the pyridine-*N* and carbonyl group of the amide moiety. Gly molecule acted as a uninegatively monodentate ligand and coordinate to the metal ions through its carboxylic group, in addition PhA acted as a uninegatively bidentate ligand and coordinate to the metal ions through its carboxylic and amino groups. All the chelates have octahedral geometrical structures while Cu(II)- and Zn(II)-ternary chelates with PhA have square planar geometrical structures. The molar conductance data reveal that most of these chelates are non electrolytes, while Fe(III)-Pir-Gly, Co(II)-, Ni(II)-, Cu(II)- and Zn(II)-Pir-PhA cheletes were 1:1 electrolytes. X-ray powder diffraction is used as a new tool to estimate the crystallinity of chelates as well as to elucidate their geometrical structures.

Keywords: Piroxicam; Ternary chelates; IR; Magnetic and diffuse reflectance spectra; UV-Vis; XRD

1. Introduction

An intensive number of studies on the formation of mixed ligand complexes reveals a realization of their growing importance, particularly in their role in biological process [1]. The formation of mixed ligand chelates is a general feature of systems where a metal is present with two or more ligands. The study of these complexes shows that their formations are a favoured process over that of simple complexes [2]. The study of ternary complexes involving an aromatic amine as the primary ligand, various amino acids (AA) and biomolecules as secondary ligands can serve as useful models for gaining a better understanding of enzyme–metal ion–substrate complexes, which play an important role in metalloenzyme-catalysed biochemical reactions [3–5]. Rheumatoid arthritis is a disease characterized by painful disorders in the muscle and joints. At present, therapeutical treatment, for this illness are mainly based on non-steroidal anti-inflammatory drugs (NSAIDs), characterized by rapid and complete uptake in the blood stream and thus possessing a fast analgesic action [6]. Piroxicam (Pir; 4-hydroxy-2-methyl-*N*-(2-pyridyl)-2H-1,2-benzothiazine-3-carboxamide 1,1-dioxide) is the most important member of oxicams class (Fig. 1) [6–10] to be strong chelators for several divalent metal ions from the 'd-block' of the periodic table, via the amide oxygen atom and nitrogen atoms from the pyridyl or thiazolyl rings [8,9]. In this type of compounds the enol oxygen atom is always deprotonated, is not linked to the metal but instead is linked to the N–H function via a strong intramolecular hydrogen bond mode possible by ZZZ conformation at the C(3)–C(4), C(14)–N(16) and N(16)–C(2′) vectors. The involvement of the enolate oxygen atom of 'oxicam' ligands in the coordination to the metals has been clearly shown only in the case of Sn(IV) complex [11] and this is related to a highly affinity of this metal ion towards the oxygen

---

* Corresponding author.

E-mail address: ggenidy@hotmail.com (G.G. Mohamed).

1386-1425/$ – see front matter © 2004 Elsevier B.V. All rights reserved.
doi:10.1016/j.saa.2004.01.035

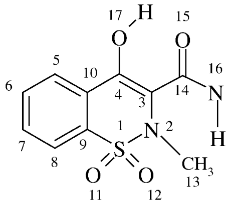

Fig. 1. Structural formula for piroxicam (H_2Pir).

donor, and to the deprotonated form of the ligand used in the preparative procedure (Pir^{2-}, H_2Pir, piroxicam) as shown in Fig. 1.

With the aim to continue the exploration of the coordination mode adopted by piroxicam we have performed a preparative and structural work by using piroxicam (as primary ligand) with various amino acids such as glycine (Gly) as an example of non-essential amino acid and DL-phenylalanine (PhA) as an example of essential amino acid (as secondary ligand) with some ‘d-block’ metal ions by employing the amide oxygen and pyridyl nitrogen of the drug molecule with deprotonated carboxylate group in unidentate manner of glycine and uninegatively bidentate through deprotonated carboxylate and amino groups of DL-phenylalanine. The solid chelates are characterized using different physico-chemical methods like IR, UV-Vis, molar conductance, magnetic moment and diffuse reflectance spectra. XRD technique is also utilized as a confirmatory tool for elucidation the crystallinity of the chelates.

2. Experimental

2.1. Materials

All chemicals used were of the analytical reagent grade (AR), and of highest purity available. They included piroxicam, an authentic sample was kindly supplied by Pfizer Company, Cairo (Egypt) and its melting point was checked (198 °C) to confirm its purity. Amino acids; DL-phenylalanine was supplied from Acros (USA), while glycine was supplied from Sigma.

Copper(II) acetate dihydrate (Prolabo); cobalt(II) and nickel(II) chlorides hexahydrate (BDH); zinc acetate dihydrate (Ubichem), anhydrous ferrous sulphate (Sigma) and ferric chloride hexahydrated (Prolabo), boric acid (BDH), phosphoric and glacial acetic acids (AR) were used. Zinc oxide, disodium salt of ethylenediaminetetraacetic acid (EDTA; Analar), ammonia solution (33% v/v) and ammonium chloride (El Nasr pharm. Chem. Co., Egypt). Absolute ethyl alcohol, diethylether, nitric acid (Analar) and dimethylformamide (DMF) were supplied from ADWIC. Hydrogen peroxide and sodium hydroxide were supplied from Prolabo. De-ionized water collected from all glass equipments was usually used in all preparations.

2.2. Instrumentation

The spectrophotometric measurements in solution were carried out using automated spectrophotometer UV/Vis Perkin-Elmer Model Lambda 20 ranged from 200 to 900 nm. Elemental microanalysis of the separated solid chelates for C, H, N, and S were performed in the Microanalytical Center, Cairo University. The analyses were repeated twice to check the accuracy of the analyses data. Infrared spectra were recorded on a Perkin-Elmer FT-IR type 1650 spectrophotometer in wavenumber region 4000–200 cm^{-1}. The spectra were recorded as KBr pellets. The solid reflectance spectra were measured on a Shimadzu 3101pc spectrophotometer. The molar magnetic susceptibility was measured on powdered samples using the Faraday method. The diamagnetic corrections were made by Pascal’s constant and $Hg[Co(SCN)_4]$ was used as calibrant.

The X-ray powder diffraction analyses were carried out by using Rigku Model ROTAFLEX Ru-200. Radiation was provided by copper target (Cu anode 2000 W) high intensity X-ray tube operated at 40 KV and 35 MA. Divergence slit and the receiving slit were 1 and 0.1, respectively. Metal contents were determined by titration against standard EDTA after complete decomposition of the complexes with aqua regia in kjeldahl flask. The water was always de-ionized obtained from Altra clear SG-Wasser aufbereitung und regenerierstation GmbH instrument.

2.3. Synthesis

A hot ethanol solution (60 °C) of the respective metal chlorides (Fe(II), Fe(III), Co(II) and Ni(II)) or acetate (Cu(II) and Zn(II)) solutions (1 mmol) in de-ionized water (25 ml) were added to 25 ml hot ethanol solution (60 °C) of Pir (0.331 g, 1 mmol) followed by addition of 25 ml 1 mmol Gly (0.075 g in de-ionized water) or 25 ml 1 mmol PhA (0.165 g in ethanol) in the molar ratio 1:1:1 (metal salt: Pir: Gly or PhA) in total volume 75 ml mixture. The resulting mixture was stirred under reflux for 30 min. The complexes were precipitated as microcrystalline powders. They were removed by filtration, washed with hot ethanol followed by diethylether and dried in a vacuum desiccator over anhydrous calcium chloride. All the complexes are coloured and received as powder. Their stoichiometries were confirmed by chemical analysis. The m.p. and analytical data are collected in Table 1.

3. Results and discussion

The purity of Pir is checked from ^{1}H NMR study (Fig. 2) where the spectrum shows a sharp singlet signals at $\delta = 8.9$ and 13.3 ppm with integrations correspond to one NH and one OH protons, respectively. Also, the spectrum shows a multiple peaks at $\delta = 7.13$–8.31 ppm and singlet sharp peak at $\delta = 2.91$ ppm with integrals correspond to eight

Table 1
Analytical and physical data of Pir chelates with Gly and PhA

Compound	Chemical formula	Colour	m.p. (°C)	Found, calcd. (%)					μ_{eff} (B.M.)	Λ_m (Ω^{-1} cm^2 mol^{-1})
				C	H	N	S	M		
[Pir]	$C_{15}H_{13}N_3O_4S$	White	198	54.50 (54.38)	3.70 (3.90)	12.34 (12.68)	9.55 (9.66)	–	–	–
[PhA]	$C_9H_{11}NO_2$	White	267 °C dec	65.60 (65.45)	6.43 (6.6)	8.60 (8.48)	–	–	–	–
[Gly]	$C_2H_5NO_2$	White	245 °C dec	32.00 (31.80)	6.80 (6.60)	18.42 (18.66)	–	–	–	–
Fe(II)-Pir-Gly	$[Fe(Pir)_2(Gly)_2]\cdot4.5H_2O$	Reddish brown	193	42.90 (43.08)	4.35 (4.54)	11.70 (11.83)	6.32 (6.76)	5.67 (5.91)	5.12	17.70
Fe(III)-Pir-Gly	$[Fe(Pir)_2(Gly)_2]Cl\cdot2H_2O$	Reddish brown	169	43.15 (43.52)	4.20 (4.05)	11.86 (11.95)	6.90 (6.82)	5.70 (5.97)	5.92	130
Co(II)-Pir-Gly	$[Co(Pir)_2(Gly)_2]\cdot4H_2O$	Orange	204	43.65 (43.35)	3.45 (3.61)	11.85 (11.90)	6.75 (6.80)	5.66 (6.27)	5.10	29.0
Ni(II)-Pir-Gly	$[Ni(Pir)_2(Gly)_2]\cdot4H_2O$	Light green	218	43.25 (43.35)	3.45 (3.60)	11.95 (11.90)	6.70 (6.80)	6.27 (6.27)	2.86	22.0
Cu(II)-Pir-Gly	$[Cu(Pir)_2(Gly)_2]\cdot1.5H_2O$	Olive green	159	46.60 (46.23)	4.55 (4.19)	12.75 (12.69)	7.35 (7.25)	7.62 (7.19)	2.0	10.1
Zn(II)-Pir-Gly	$[Zn(Pir)_2(Gly)_2]\cdot2H_2O$	Lemon	223	44.40 (44.31)	4.10 (4.17)	12.30 (12.29)	6.98 (7.02)	7.14 (7.28)	Diam.	25.0
Fe(II)-Pir-PhA	$[Fe(Pir)(PhA)(H_2O)_2]0.5SO_4$	Reddish brown	200	45.50 (45.35)	4.21 (4.25)	8.60 (8.82)	7.72 (7.56)	8.29 (8.82)	4.91	156
Fe(III)-Pir-PhA	$[Fe(Pir)(PhA)Cl_2]\cdot H_2O$	Reddish brown	218	44.95 (45.00)	3.90 (4.06)	8.70 (8.75)	4.90 (5.00)	4.52 (4.38)	5.70	15.70
Co(II)-Pir-PhA	$[Co(Pir)(PhA)(H_2O)_2]Cl$	Orange	140	46.12 (46.06)	4.45 (4.30)	8.85 (8.95)	5.40 (5.12)	9.60 (9.43)	5.40	115
Ni(II)-Pir-PhA	$[Ni(Pir)(PhA)(H_2O)_2]Cl$	Light green	175	46.25 (46.04)	4.48 (4.30)	8.87 (8.95)	5.25 (5.11)	9.27 (9.43)	3.40	105
Cu(II)-Pir-PhA	$[Cu(Pir)(PhA)](Ac)\cdot H_2O$	Olive green	170	46.20 (49.09)	4.45 (4.40)	8.75 (8.81)	5.25 (5.03)	9.36 (9.99)	1.70	120
Zn(II)-Pir-PhA	$[Zn(Pir)(PhA)(H_2O)_2](Ac)\cdot H_2O$	Lemon	220	46.40 (46.36)	4.80 (4.90)	8.44 (8.32)	4.60 (4.75)	9.32 (9.66)	Diam.	135

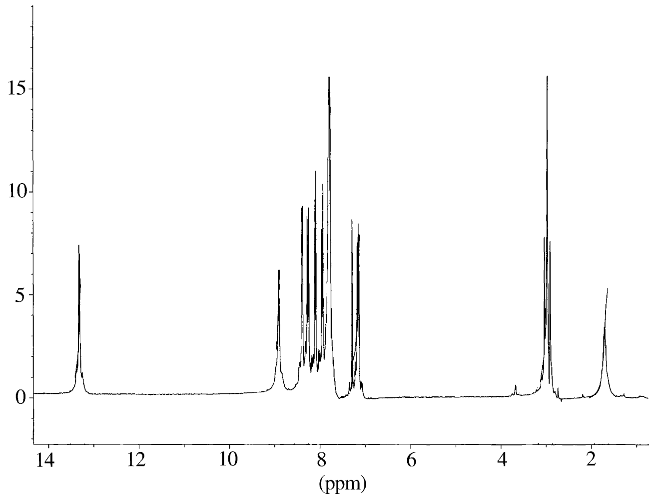

Fig. 2. ^{1}H NMR spectrum of piroxicam.

ArHs and three CH_3 protons, respectively. Due to the lack of solubility of Zn(II)-ternary chelates in different solvents, render it difficult to carry out their ^{1}H NMR spectra. The results of the elemental analyses of ternary chelates are listed in Table 1. The results are close to each other and they are in the acceptable range of ±0.5% error. It was seen from Table 1 that ternary chelates of di- and trivalent transition metals with Pir and Gly are formed with 1:2:2 ratio (metal salts: Pir: Gly). The divalent metal chelates have the general formula $[M(H_2L)_2(Gly)_2]\cdot yH_2O$ where M = Fe(II), Co(II), Ni(II), Cu(II) and Zn(II) and $y = 2 - 4$; while Fe(III)-ternary chelate has the formula $[Fe(H_2L)_2(Gly)_2]Cl\cdot 2H_2O$. The mixed ligand complexes of Pir and PhA with the same transition metals are formed with 1:1:1 ratio [metal salts: Pir: PhA]. The Fe(II), Co(II), Ni(II), Cu(II) and Zn(II)-ternary chelates have the formula $[M(H_2L)(PhA)(H_2O)_x](A)\cdot H_2O$ where A = acetate in case of Cu(II) ($x = 0$) and Zn(II) ($x = 2$); sulphate in case of Fe(II) ($x = 2$) or Cl^- in case of Co(II) ($x = 2$) and Ni(II) ($x = 2$); whereas in case of Fe(III)-ternary chelate, it has the formula $[Fe(H_2L)(PhA)(Cl)_2]\cdot H_2O$.

3.1. *UV-Vis spectra of ternary chelates*

Figs. 3 and 4 show the absorption spectra of piroxicam ternary chelates with glycine and phenylalanine, respectively, in absolute ethanol at wavelength ranging from 200 to 600 nm against the same solvent as a blank. It was shown that Pir gives three maximum bands at 205, 256 and 360 nm and shoulder band at 291 nm. While Gly and PhA exhibit three maximum bands at 204–207, 258–259 and 362–370 nm and one shoulder band at 291 nm. The higher energy band at 204–207 nm may be attributed to σ–σ^* transition ($\epsilon = 2.1$–$4.4 \times 10^5\,l\,mol^{-1}\,cm^{-1}$) while the lower energy bands ($\lambda = 256$–259 nm) can be assigned to n–π^* and π–π^* transitions ($\varepsilon = 7$–$15 \times 10^4\,l\,mol^{-1}\,cm^{-1}$) within Gly and PhA molecules.

It is obvious from the absorption spectra obtained that all the ternary chelates of Pir with Gly or PhA give the same behaviour. The first and second bands in Pir, Gly and PhA at 204–507 and 256–259 nm remain in the same position in all the chelates indicating that they are not affected by metal chelation. Moreover, they may be attributed

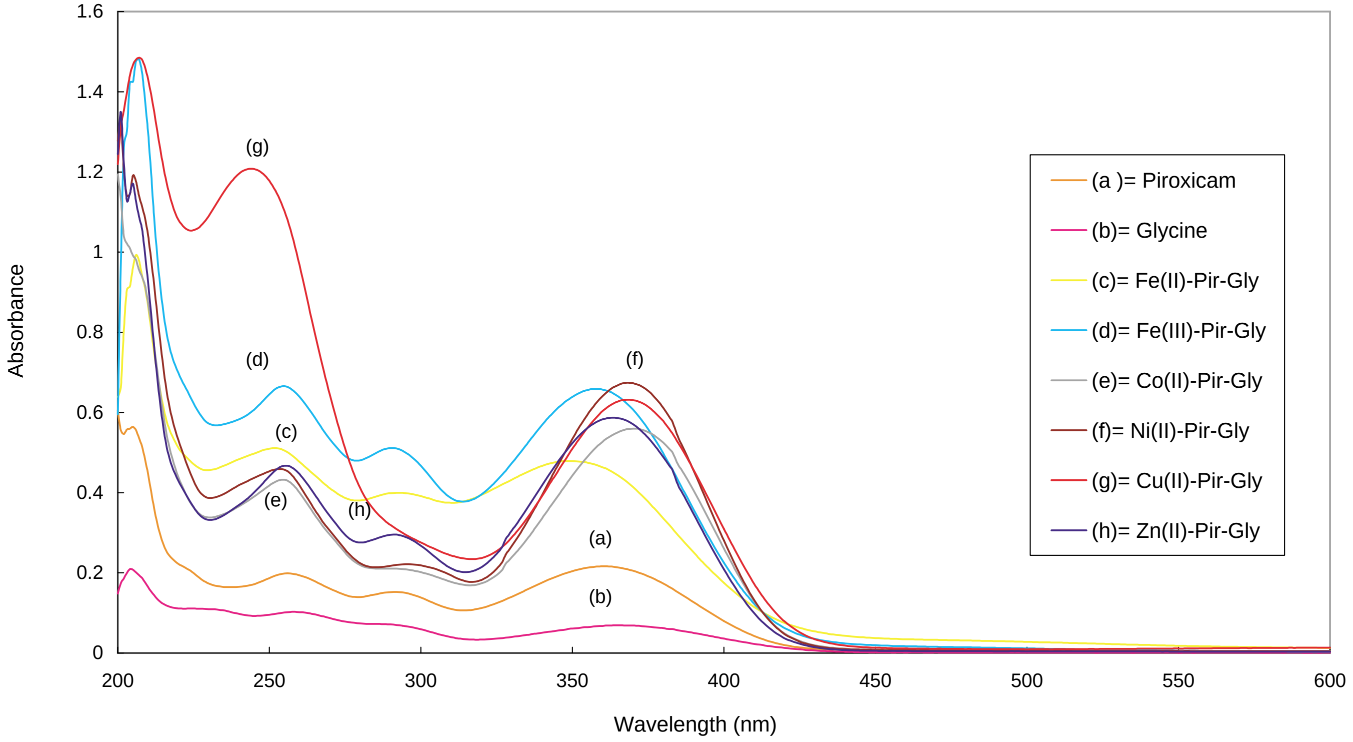

Fig. 3. Absorption spectra of piroxicam and its ternary complexes with glycine in absolute ethanol.

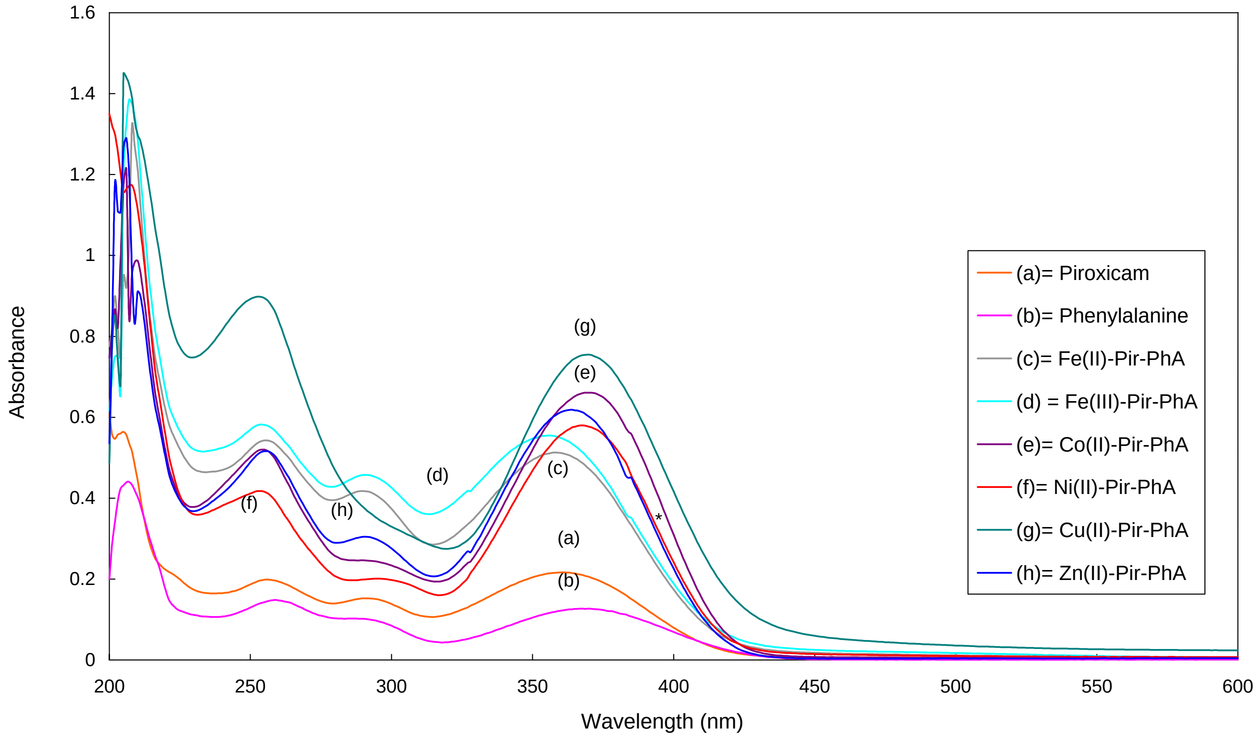

Fig. 4. Absorption spectra of piroxicam and its ternary complexes with DL-phenylalanine in absolute ethanol.

to π–π* and n–π* transition within the Pir, Gly or PhA molecules.

The shoulder band observed at 291 nm in ethanol solvent Figs. 3a and 4a may be assigned to n–π* transition within the C=O group of the amide moiety in the free Pir or carboxylate of amino acids. This band is red shifted to 292, 293, 295 nm in case of Fe(II), Fe(III) and Ni(II) chelates, while it disappeared in all the remaining chelates revealing the involvement of the C=O of amide group or carboxylate–O in chelate formation [12].

The n–π* transitions within the Pir molecule are overlapped with those of Gly and PhA molecules at $\lambda = 360–370$ nm so renders it difficult to attribute the blue or red shift of these bands as a result of the involvement of the pyridyl-N of Pir or amino group of Gly or PhA during chelate formation (N → M) [12].

3.2. IR spectra and mode of bonding

The careful inspection of the IR spectra of free Pir and its ternary complexes, is based on some general references [13] and made in comparison with other related molecules and complexes. Table 2 shows the measured IR band positions of the ternary chelates in order to facilitate the assignment of these bands in the free ligands and their metal chelates.

Figs. 5 and 6 show the IR spectra of Pir and its ternary chelates with Gly and PhA, respectively, at the wavenumber range 4000–200 cm^{-1}.

The well-defined peaks at 3385 s and 3336 s cm^{-1} in the spectrum of Pir are assigned to the ν(N–H) and ν(O–H) vibrations, respectively. The other series of weak bands between 3100 and 2800 cm^{-1} are related to (C–H) modes of vibrations. After complexation, the full region is dominated by two strong broad bands related to the stretching modes of the water molecules. Some weak bands are located between 2000 and 1700 cm^{-1} and can be assigned to overtones of the aromatic rings.

In the wavenumber range 1700–1000 cm^{-1} some of the most characteristic bands of these systems are found. The so-called amide I band, which represents mainly the ν(C=O) stretching mode, is seen as a very strong band at 1630 cm^{-1}, with a weak shoulder at 1612 cm^{-1} in free Pir. In Pir complexes, this band is shifted to higher or lower frequencies or disappear (see Table 2), supporting the participation of the carbonyl group of the Pir in the metal coordination [14]. This band appears broadened in most of the chelates by the simultaneous appearance of the $\delta(H_2O)$ vibration in the same range, a fact which obstructs the clear visualization of the effective displacement of the ν(C=O) band [9]. Another band vibration $\nu(CN) + \delta(NH)$ combination usually known as amide III, can be assigned to the strong band seen at 1301 cm^{-1} in Pir, which is absent in the spectra of the complexes, or it may be shifted and superimposed on any other near-lying band. As it known, this band is very sensitive to the geometrical changes in the O=C–N(H)–C moiety [15]. Since after complexation, the carbonyl group is involved in coordination, such changes are, obviously, important in this part of the Pir molecule.

The band located at 1572 cm^{-1} is assigned to the ν(C=N) stretching vibration of pyridyl nitrogen. This band disap-

Table 2
IR assignment (4000–200 cm^{-1}) of Pir ternary metal chelates with Gly and PhA

	ν_{asym}(COO)	ν_{sym}(COO)	δNH_2	ν(CONH)	ν(C=N)	ρ(py)	$\nu_{asym}(SO_2)$	$\nu_{sym}(SO_2)$	ν(M–N)	ν(M–O)	ν(M–O) (Gly)	ν(M–O) (PhA)	ν(M–N) (PhA)
(PhA)	1586 s	1412 s	1502 s	–	–	–	–	–	–	–	–	–	–
(Gly)	1594 s	1408 s	1524 s	–	–	–	–	–	–	–	–	–	–
(Pir)	–	–	–	1630 s	1572 m	623 s	1351 s	1040 m	–	–	–	–	–
Fe(II)-Pir-Gly	1597 w	1401 m	1516 w	dis	dis	673 m	1325 m	1063 w	570 w	375 w	410 w	–	–
Fe(III)-Pir-Gly	1562 s	1429 m	1524 w	1602 m	dis	670 w	1349 m	1045 w	578 w	381 w	336 w	–	–
Co(II)-Pir-Gly	1548 w	1391 m	1528 w	dis	dis	659 w	1326 w	1037 w	570 s	386 w	454 w	–	–
Ni(II)-Pir-Gly	1584 br	1401 s	1518 m	dis	dis	672 w	1325 w	1061 w	568 w	376 m	338 w	–	–
Cu(II)-Pir-Gly	1575 br	1396 m	1518 m	dis	dis	658 w	1331 w	1055 m	566 m	374 w	333 w	–	–
Zn(II)-Pir-Gly	1587 br	1402 w	1517 m	dis	dis	673 m	1327 m	1065 m	569 w	379 m	355 w	–	–
Fe(II)-Pir-PhA	1580 br	1397 w	1520 w	dis	dis	670 w	1328 w	1040 w	573 w	358 w	–	433 w	331 w
Fe(III)-Pir-PhA	1605 m	1400 w	1525 m	dis	dis	650 w	1326 w	1038 w	576 w	363 w	–	410 w	334 w
Co(II)-Pir-PhA	1580 w	1399 m	1516 m	dis	dis	650 w	1326 w	1065 w	573 w	357 w	–	430 w	332 w
Ni(II)-Pir-PhA	1588 br	1400 m	1516 m	dis	dis	670 m	1327 m	1063 m	570 w	372 m	–	433 w	337 w
Cu(II)-Pir-PhA	1574 w	1391 m	1518 m	dis	dis	666 w	1333 m	1055 w	568 w	375 w	–	437 w	324 w
Zn(II)-Pir-PhA	1575 w	1397 w	1514 w	1621 w	dis	656 w	1330 w	1048 w	566 w	357 w	–	425 w	313 w

s: strong; w: weak; m: medium; br: broad; dis: disappear.

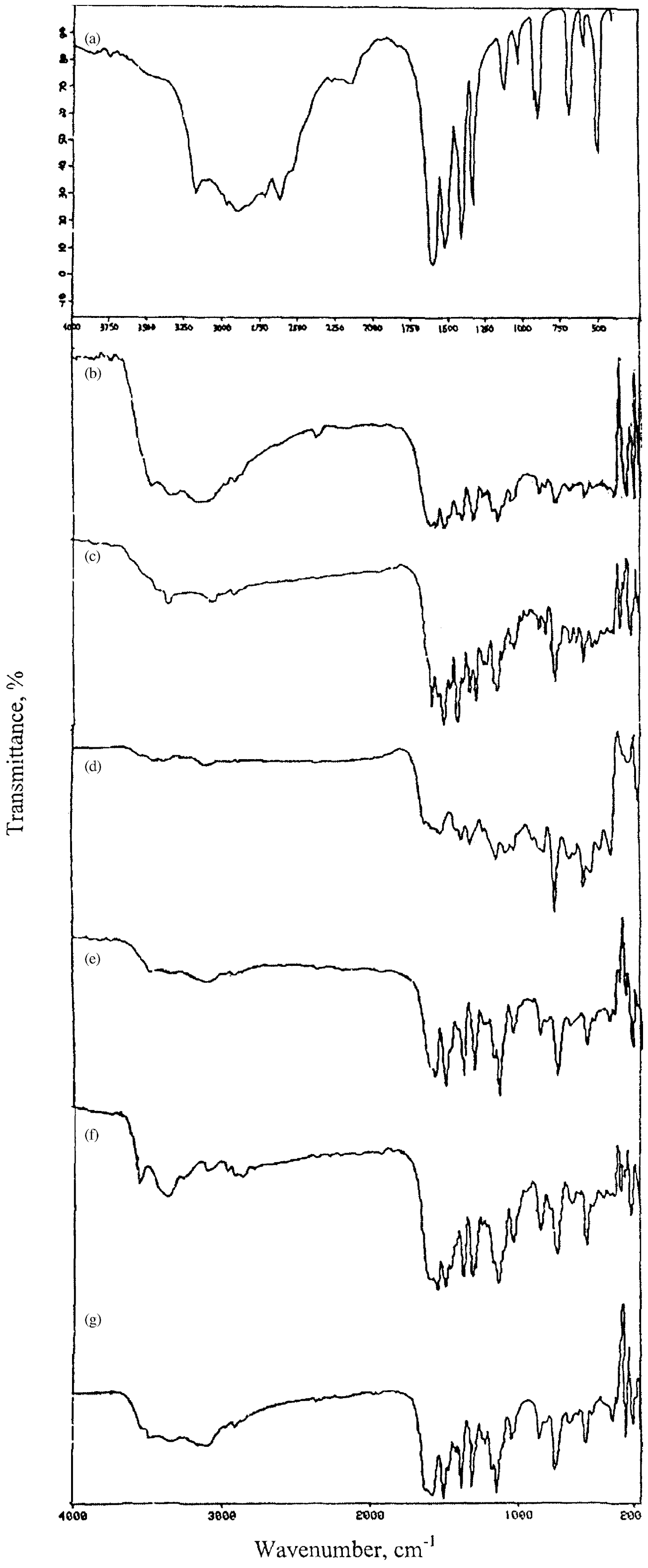

Fig. 5. IR spectra (4000–200 cm^{-1}) of Pir and Gly mixed ligand chelates: (a) Gly, (b) Fe(II), (c) Fe(III), (d) Co(II), (e) Ni(II), (f) Cu(II) and (g) Zn (II).

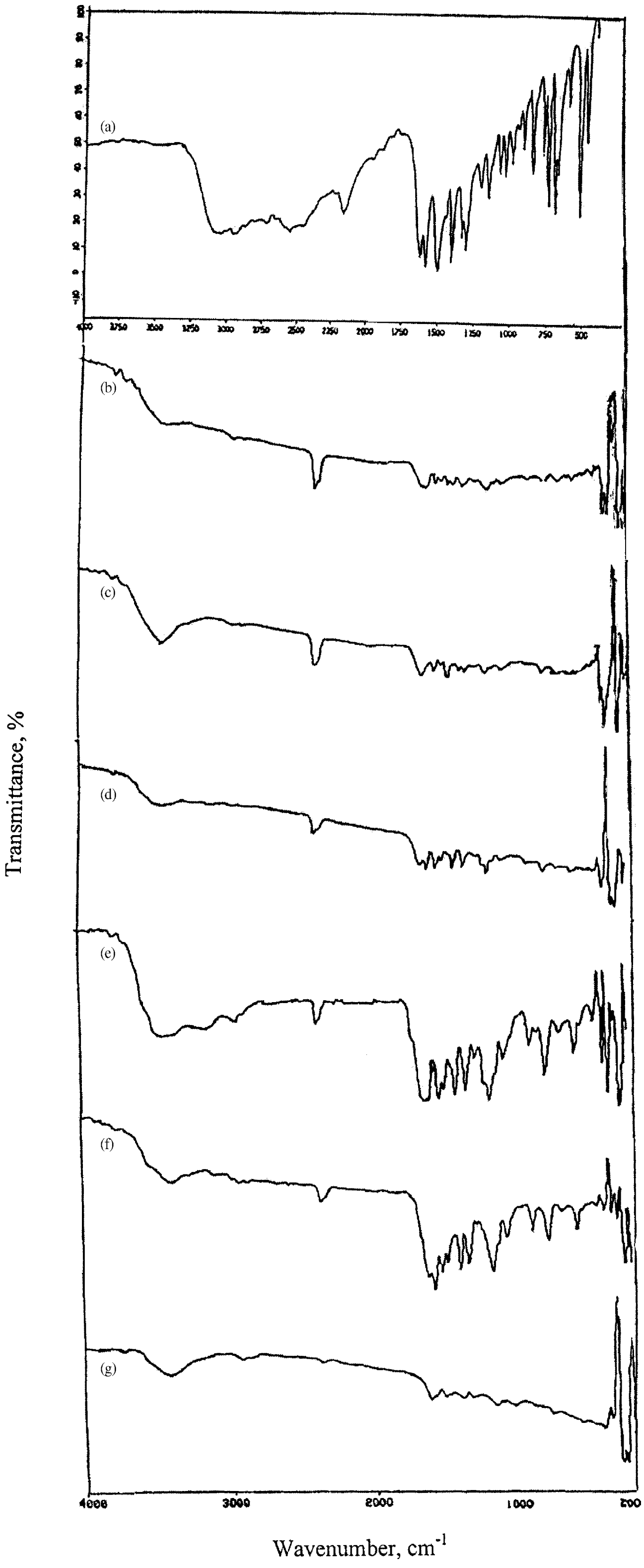

Fig. 6. IR spectra (4000–200 cm^{-1}) of Pir and PhA mixed ligand chelates: (a) PhA, (b) Fe(II), (c) Fe(III), (d) Co(II), (e) Ni(II), (f) Cu(II) and (g) Zn(II).

peared but it is still difficult to confirm the participation of the pyridyl nitrogen as its band overlapped with those of the carboxylate group of the amino acids or the amide II stretching vibration band. Its participation is confirmed from the band due to in-plane deformation ρ(py) located at 600 and 400 cm^{-1}.

The in-plane ring deformation (604 cm^{-1} in free pyridine) is probably overlapped by the 623 cm^{-1}. After complexation, the band at 623 cm^{-1} disappears and a new band at 673–650 cm^{-1} is found in the ternary chelates, as previously reported for pyridine complexes of divalent ions of the first row transition metal series [16]. Detecting the shift of the out-of-plane ρ(py) at 405 cm^{-1} is difficult because the spectra are rich for the complexes.

Two bands, located at 1351 and 1040 cm^{-1}, are assigned to the antisymmetric and symmetric stretching vibrations of the SO_2 group, respectively. Interestingly, these bands are found in particularly the same position as in saccharin [17], a molecule with a structure very similar to that of the benzothiazine part of Pir. These two SO_2 bands are shifted to lower or higher frequencies in ternary complexes, in accordance to the assignment of Cini et al. [8]. As the SO_2 group is not involved in metal binding, this shift to higher frequencies must be related to important hydrogen bonding effects. Another possible explanation for this shift may be due to the electronic density changes on the sulfur atom and in the ring after complex formation.

Most of the band shifts observed at the wavenumber region 1150–994 cm^{-1} are in agreement with the structural changes observed in the molecular carbon skeleton after complexation, which cause some important changes in (C–C) bond lengths and also affect some of the C–O and C–N bonds indirectly [6].

The bands between 840 and 732 cm^{-1} can be assigned to δ(CH) and to ring modes, respectively. One group of interesting bands of the free ligand in this region are those located at 691 and 623 cm^{-1}. The first of them may be the so-called amide V band [(mainly out-of-plane δ(NH)]. The second may be attributed to the δ(OCN) (amide IV) and the δ(CO) out-of-plane (amide VI) modes as well as internal pyridine modes. Both groups of bands change appreciably after complexation. The Pir bands found at 938, 831 and 732 cm^{-1} also disappear or shifted to higher wavenumbers after complexation. Some of them are surely related to complicated skeletal modes involving vibrations of the –C(O)-NH- portion of the molecule [9].

The bands at the wavenumber 1594–1586 and 1412–1408 cm^{-1} regions, in the free amino acids; Gly or PhA, are assigned to the antisymmetric and symmetric stretching vibrations of the carboxylate group, respectively. The shift of these two bands to higher or lower frequencies suggest the participation of –COOH group in complex formation after deprotonation [18]. The values of band shift $\Delta\nu$ (ν_{as}(COO)–ν_{sym}(COO)) are all about 143–205 cm^{-1}, indicating that the carboxylate group in both Gly and PhA are chelated in a unidentate manner to the metal ions [18].

At the wavenumber 3500–3000 cm^{-1} region of the ternary chelates of Pir, the overlap of the various ν(NH) vibrations coupled in many cases with molecules of water of hydration gives rise to very strong absorption. This prevents the individual recognition of the various bands. The band due to the in-plane deformation of the amino group of Gly (δNH_2) at 1524 cm^{-1} is slightly shifted to higher or lower frequencies (1528–1516 cm^{-1}) upon chelation indicating non-participation of the nitrogen atom in bonding to the metal ions. The shift to higher or lower wavenumbers may be attributed to the participation of the NH_2 group in intramolecular hydrogen bond. The band due to δNH_2 of DL-phenylalanine appeared as a maximum near 1502 cm^{-1}. This band has been shifted to the extent 12–23 cm^{-1} in all the complexes confirming coordination of the NH_2 group to the metal ions [19,20].

The ν(M–N) bands for the pyridyl nitrogen appeared in the wavenumber range 566–573 cm^{-1} for the divalent and at 576–578 cm^{-1} for the trivalent metal ion [16]. New peaks of weak or medium intensity are observed in the wavenumber range 357–386 cm^{-1} which are attributed to ν(M–O) vibrations of ternary chelates [21]. The band at 334 cm^{-1} is assigned to the M–Cl vibration of Fe(III) ternary complex with Pir and PhA [22]. The stretching vibration bands due to ν(M–O) of amino acids (Gly and PhA) appeared in the region of 454–313 cm^{-1}, as reported for $[Cu(Gly)_2]$ and $[Cu(ala)_2]$ complexes [23]. While the ν(M–N) bands [23] of the PhA ternary chelates are observed in the region 410–437 cm^{-1}.

The vibrations of the sulphate ion in Fe(II)-ternary chelates with PhA appears at 1160 and 629 cm^{-1}. This in association with conductance data indicate the uncoordinated nature of sulphate group [24].

Therefore, it is concluded that from UV-Vis and IR spectra that Pir behaves as neutral bidentate ligand coordinated to the metal ions through amide–CO and pyridine-*N*. In addition, Gly is bonded to the metal ions through its deprotonated carboxylate group in unidentate manner, while the amino group is remained unchanged in the ternary chelates. In the case of DL-phenylalanine, it behaves as a uninegatively bidentate ligand where it binds to the central metal ions through its deprotonated carboxylate group and its amino group. Hence, these studies, IR and UV-Vis, give us useful information's about how Pir appear its effect with Gly or PhA on metal ions present in the biological fluids in the human body.

3.3. *Molar conductivity measurements*

As seen from Table 1, the molar conductivity value of Fe(III)-Pir-Gly is 130 Ω^{-1} cm^2 mol^{-1}. Furthermore the molar conductivity of the most of Pir-PhA chelates are found to be 156, 115, 105, 120 and 135 Ω^{-1} cm^2 mol^{-1} for Fe(II), Co(II), Ni(II), Cu(II) and Zn(II)-chelates, respectively. It is obvious from the data that these complexes are ionic in nature and they are of the type 1:1 electrolytes [25]. On the other hand; the remaining chelates have molar conductivity values ranged from 10.1 to 29.0 Ω^{-1} cm^2 mol^{-1}. These values indicate the non-ionic nature of these chelates and they are considered as non electrolytes [25]. Hence, the molar conductance measurements of the chelates confirm the proposed general formulae of those chelates as suggested depending upon the results of elemental analyses and IR spectra.

3.4. *Magnetic susceptibility and electronic spectra*

As further structural tools, magnetic and solid reflectance spectral studies have been used to confirm the geometry of the complexes. From the diffuse reflectance spectra it is observed that, the ternary Fe(III)-chelates exhibit a band at (21.93–21.14) × 10^3 cm^{-1}, which may be assigned to the $^6A_{1g} \rightarrow T_{2g}$ (G) transition in octahedral geometry of the complexes. The $^6A_{1g} \rightarrow {}^5T_{1g}$ transition appears to be split into two bands at (12.42–11.90) × 10^3 cm^{-1} and (8.98–17.61) × 10^3 cm^{-1}. The observed magnetic moments of Fe(III) complexes are 5.7–5.92 B.M. Thus, the complexes formed have the octahedral geometry involving d^{2}sp^3 hybridization in Fe(III) ion [26].

The diffused reflectance spectra of mixed ligand complexes of Fe(II) ion display two absorption bands at (12.20–11.63) × 10^3 cm^{-1} and (22.22–17.73) × 10^3 cm^{-1} which are assigned to $^5T_{2g} \rightarrow {}^5E_g$ transition and charge transfer, respectively [27]. The Fe(II) chelates exhibit magnetic moment values of 4.91–5.12 B.M., which are consistent with a high spin octahedral geometry [28]. The Ni(II)-mixed ligand complexes of Pir and Gly or PhA reported herein are high spin with a room temperature magnetic moment values of 2.86–3.40 B.M.; which are in the normal range observed for octahedral Ni(II)-complexes [27]. This indicates that, the mixed ligand complexes of Ni(II) are six coordinate and probably octahedral [29].

Their electronic spectra, in addition to show the π–π* and n–π* bands of free ligands, display three bands, in the solid reflectance spectra at:

$$\nu_1 : (12.63\text{–}11.61) \times 10^3\,\text{cm}^{-1} : {}^3A_{2g} \rightarrow {}^3T_{2g}$$

$$\nu_2 : (15.77\text{–}14.64) \times 10^3\,\text{cm}^{-1} : {}^3A_{2g} \rightarrow {}^3T_{1g}(\text{F})$$

$$\nu_3 : (20.28\text{–}19.08) \times 10^3\,\text{cm}^{-1} : {}^3A_{2g} \rightarrow {}^3T_{1g}(\text{P})$$

The Racah parameters are calculated according to the following equations:

$$B = \frac{\nu_2 + \nu_3 - 3\nu_1}{15}$$

$$B = \frac{1}{75}\{3\nu_2[25(\nu_3 - \nu_2)^2 - 16\nu_1]^2\}^{1/2}$$

$$10\text{Dq} = \nu_1$$

The 10Dq values lie in the 11.61–12.63 × 10^3 cm^{-1} range, again confirming the octahedral configuration of the Ni(II) chelates [29]. The smaller *B* values (560–820 cm^{-1}) compared to the free metal ion (1080 cm^{-1}) are due to the strong interaction between the reactive sites of the organic compounds with nickel. The *B* values are less than unity (0.52–0.76), suggesting a largely covalent bond between the organic ligand and nickel. The electronic spectra of the ternary Co(II)-complexes give three bands at (12.27–11.31) × 10^3 cm^{-1}, (15.04–13.89) × 10^3 cm^{-1} and at (17.59–16.34) × 10^3 cm^{-1} wavenumber regions, respectively. The third region (18.18–26.06) × 10^3 cm^{-1} refers to the charge transfer band. The bands observed are assigned to the transitions $^4T_{1g}(\text{F}) \rightarrow {}^4T_{2g}(\text{F})(\nu_1)$, $^4T_{1g}(\text{F}) \rightarrow {}^4A_{2g}(\text{F})(\nu_2)$ and $^4T_{1g}(\text{F}) \rightarrow {}^4T_{2g}(\text{P})(\nu_3)$, respectively, suggesting that there is an octahedral geometry around Co(II) ion [30,31]. The ratio $\nu_3/\nu_1 = 1.14$–1.58 is lower than the expected for octahedral Co(II)-complexes (1.95–2.48) [32].

For calculating the Racah parameters, the following two equations are used [39]:

$$10\text{Dq} = 2\nu_1 - \nu_3 + 15B$$

$$B = \frac{1}{30}[-(\nu_1 - \nu_3) \pm (-\nu_1^2 + -\nu_3^2 + \nu_1\nu_3)^{1/2}]$$

$$10\text{Dq} = \frac{1}{3}(2\nu_2 - \nu_3) + 5B$$

$$B = \frac{1}{510}[7(\nu_3 - 2\nu_2) \pm 3[81\nu_3^2 - 16\nu_2(\nu_2 - \nu_3)^{1/2}]$$

The *B* parameter is a measure of the electron–electron repulsion term, which is lower in the complexes (600–850 cm^{-1}) than in free ion (985 cm^{-1}), with *B* values in the 0.61–0.86 range. From the position of the bands and the calculated Racah parameters, the chelates are octahedral with largely covalent bonds between the organic ligands and the metal ion [30]. The magnetic susceptibility measurements lie in the 5.4–5.1 B.M. range (normal range for octahedral Co(II)-complexes is 4.3–5.2 B.M.), is an indicative of octahedral geometry [32].

The reflectance spectra of Cu(II)-ternary chelates with Pir in the presence of Gly consist of a broad, low intensity shoulder band centered at 17.86 × 10^3 cm^{-1} that forms part of the charge transfer band. The ^2E_g and $^2T_{2g}$ states of the octahedral copper(II) ion (d^9) split under the influence of the tetragonal distortion and the distortion can be such as to cause the three transitions $^2B_{1g} \rightarrow {}^2B_{2g}$; $^2B_{1g} \rightarrow {}^2E_g$ and $^2B_{1g} \rightarrow {}^2A_{1g}$ to remain unresolved in the spectra [33]. It is concluded that, all three transitions lie within the single broad envelope centered at the same range previously mentioned. The magnetic moment of 2.0 B.M. falls within the range normally observed for octahedral Cu(II)-complexes [34]. While the Cu(II)-complexes of Pir ternary chelates in the presence of PhA exhibit a broad band in the region 16.67 × 10^3 cm^{-1} assigned to $^2E_g \rightarrow {}^2T_{2g}$ transition and broad band in the region 14.71 × 10^3 cm^{-1} which is assigned to $^2B_{1g} \rightarrow {}^2A_{1g}$ as well as a shoulder band in the range 17.61 × 10^3 cm^{-1} characteristic of a square planner geometry for Cu(II) complexes with $d_{x^2-y^2}$ ground state [35]. The magnetic moments of the Cu(II)-complexes are found to be 1.7 B.M., a dsp^2 hybrid orbital being involved [35]. A moderately intense peak

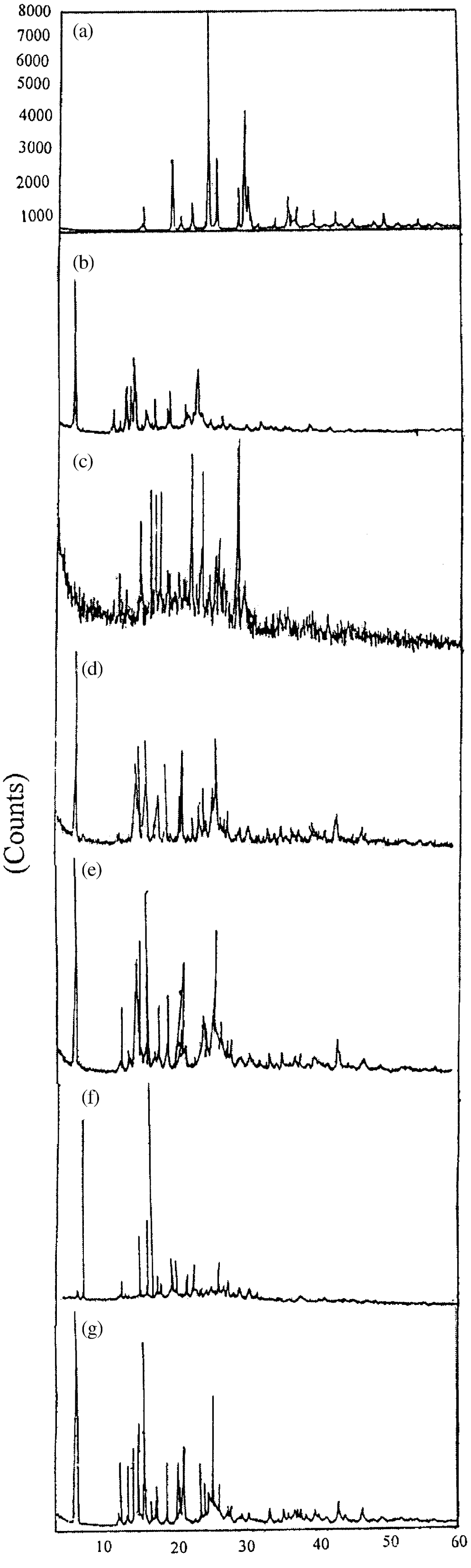

Fig. 7. X-ray diffraction pattern of Pir and Gly mixed ligand chelates: (a) Gly, (b) Fe(II), (c) Fe(III), (d) Co(II), (e) Ni(II), (f) Cu(II) and (g) Zn (II).

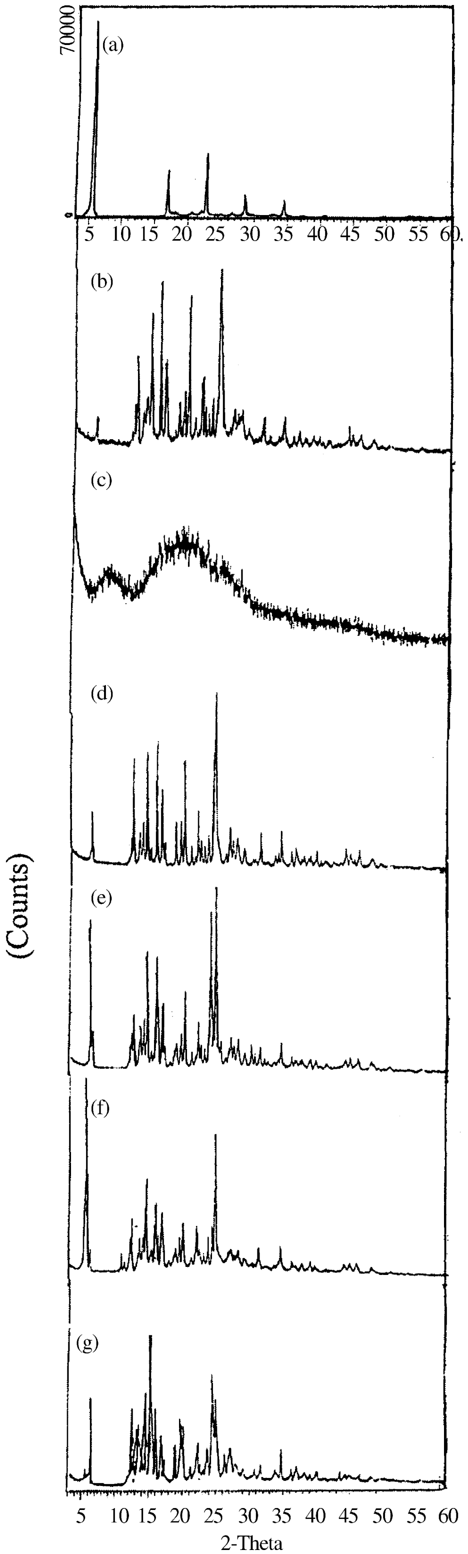

Fig. 8. X-ray diffraction pattern of Pir and PhA mixed ligand chelates: (a) PhA, (b) Fe(II), (c) Fe(III), (d) Co(II), (e) Ni(II), (f) Cu(II) and (g) Zn (II).

Table 3
Characteristic lines of X-ray powder diffraction of Gly and its ternary chelates with Pir

Compound	d (Å)	2θ	I/I_0
Glycine (Gly)	5.99	14.78	11.36
	4.68	18.94	32.25
	4.41	20.10	6.19
	4.09	21.73	12.43
	3.72	32.92	100.0
	3.52	25.29	32.24
	3.14	28.43	18.35
	3.05	29.29	53.95
	2.99	29.81	19.58
	2.53	35.38	14.78
	2.45	36.62	9.41
	2.31	39.04	8.52
	1.86	48.98	6.60
	1.69	53.94	2.66
$[Fe(II)(Pir)_2(Gly)_2]\cdot 4.5H_2O$	15.33	5.76	100
	6.41	13.80	27
	6.02	14.70	30
	5.80	15.26	48
	5.18	17.10	15
	4.79	18.50	20
	4.25	20.88	27
	3.81	23.34	15
	3.52	25.28	36
$[Fe(II)(Pir)_2(Gly)_2]Cl\cdot 2H_2O$	8.08	10.93	27
	7.60	11.63	38
	6.08	14.54	63
	5.51	16.06	76
	5.27	16.79	71
	5.06	17.49	76
	4.68	18.92	38
	4.38	20.20	37
	4.23	20.95	37
	4.12	21.54	31
	4.06	21.86	92
	3.83	23.18	50
	3.80	23.38	83
	3.44	25.84	50
	3.34	26.60	38
	3.13	28.43	100
	3.02	29.50	35
	2.97	30.04	21
$[Co(II)(Pir)_2(Gly)_2]\cdot 4H_2O$	15.52	5.68	100
	13.12	6.73	11
	7.41	11.93	35
	6.22	14.23	47
	6.03	14.67	55
	5.27	16.70	17
	5.10	17.36	28
	4.79	18.47	43
	4.26	20.82	47
	3.78	23.49	27
	3.46	25.71	53
	3.24	27.49	21
$[Ni(II)(Pir)_2(Gly)_2]\cdot 4H_2O$	15.56	5.67	100
	7.40	11.95	36
	6.83	12.96	13
	6.26	14.10	57
	6.07	14.58	65
	5.70	15.52	90
	5.13	17.27	36
	4.79	18.50	39
	4.37	20.32	34
	4.26	20.83	52
	3.81	23.34	26
	3.77	23.57	30
	3.56	25.01	30
	3.49	25.52	68
	3.41	26.14	28
	3.23	27.55	19
	2.12	42.71	18
$[Cu(II)(Pir)_2(Gly)_2]\cdot 1.5H_2O$	13.94	6.34	86
	7.36	12.02	11
	6.96	12.70	7
	6.08	14.75	30
	5.68	15.75	100
	5.13	17.24	15
	5.01	17.69	11
	4.63	19.13	23
	4.49	19.74	23
	3.95	22.43	16
	3.58	24.87	10
	3.43	25.92	21
	2.95	30.28	10
	2.84	31.47	7
$[Zn(II)(Pir)_2(Gly)_2]\cdot 2H_2O$	15.43	5.72	100
	7.44	11.89	29
	6.41	13.80	38
	6.10	14.50	51
	5.81	15.24	91
	4.80	18.50	29
	4.36	20.33	22
	4.25	20.87	38
	3.80	23.40	27
	3.54	25.10	56
	3.42	26.00	20

Table 3 (*Continued*)

Compound	d (Å)	2θ	I/I_0	Compound	d (Å)	2θ	I/I_0
	2.93	30.39	15				
	2.28	39.40	17				
	2.11	42.72	21				
	1.96	46.32	15				

Table 4
Characteristic lines of X-ray powder diffraction of PhA and its ternary chelates with Pir

Compound	d (Å)	2θ	I/I_0	Compound	d (Å)	2θ	I/I_0
DL-Phenylalanine (PhA)	15.72	5.62	100	[Ni(II)(Pir)(PhA) $(H_2O)_2$]Cl	15.38	5.74	100
	5.21	17.00	23		7.37	12.00	28
	3.90	22.76	33		6.29	14.06	49
	3.12	28.56	12		6.04	14.66	59
	2.60	34.48	10		5.73	15.46	91
					5.13	17.28	30
					4.78	18.56	32
					4.24	20.92	41
					3.50	25.44	61
					3.40	26.18	19
					3.28	27.16	10
					2.95	30.30	8
					2.50	35.96	8
					2.10	42.94	10
[Fe(II)(Pir)(PhA)$(H_2O)_2$]0.5SO_4	15.40	5.72	100	[Cu(II)(Pir)(PhA)$(H_2O)_2$](Ac)·H_2O	16.47	5.36	53
	6.13	14.44	27		15.82	5.58	27
	6.04	14.66	50		13.97	6.32	100
	5.78	15.32	50		6.09	14.54	24
	5.14	17.22	20		5.69	15.56	75
	4.91	18.06	16		4.63	19.14	15
	4.80	18.46	39		4.49	19.76	14
	4.26	20.84	36		3.95	22.46	13
	3.51	25.38	29		3.43	25.92	14
	3.38	26.28	18		3.26	27.32	8
	3.25	27.40	11		3.07	28.98	4
[Fe(III)(Pir)(PhA)$(Cl)_2$]·H_2O	–	–	–	[Zn(II)(Pir)(PhA)$(H_2O)_2$](Ac)·H_2O	16.85	5.24	61
					15.54	5.68	100
					7.45	11.86	28
					6.41	13.80	38
					6.10	14.50	52
					5.81	15.24	87
					4.26	20.84	33
					3.80	23.38	24
					3.55	25.10	44
					3.43	25.98	16
[Co(II)(Pir)(PhA)$(H_2O)_2$]Cl	15.49	5.70	100				
	6.37	13.88	14				
	6.04	14.66	16				
	5.77	15.34	27				
	5.13	17.26	15				
	4.25	20.86	18				
	3.80	23.38	15				
	3.51	25.34	17				
	3.48	25.54	12				
	2.55	35.14	11				
	2.1	43.02	7				

observed in the range (33.56–27.17) × $10^3\,\text{cm}^{-1}$ is due to ligand–metal charge transfer transition [36].

In analogy with those described for Zn(II) complexes containing N–O donor Schiff bases [37–39] and according to the empirical formulae of these complexes, we proposed an octahedral geometry for the mixed ligand Zn(II)-complexes of Pir (as primary ligand) and Gly or PhA (as secondary ligands) with two axial position occupied by the two glycine molecules or water molecules in case of Pir mixed ligand complexes with PhA.

3.5. *X-ray powder diffraction*

Figs. 7a and 8a show the X-ray powder diffraction pattern of Gly and PhA, respectively. The values of 2θ, interplanar distance (d, Å and $(I/I_0) \times 100$ are listed in Tables 3 and 4.

Form the obtained X-ray chart and interplanar distance (d, Å) values, it is obvious that Gly exists as α-Gly form while PhA exists as DL-phenylalanine form, in accordance with the previously reported data [40,41]. The space group of Gly (monoclinic $P2_1/n$ (14)) and PhA (orthorhombic P212121 (19), are determined.

Figs. 7 and 8 show the X-ray powder diffraction spectra of ternary chelates under study. Tables 3 and 4 illustrate the X-ray diffraction pattern for ternary chelates with their characteristic d-spacing (Å), 2θ and relative intensity $(I/I_0 \times 100)$. The d-spacing (Å) and $(I/I_0 \times 100)$ of these ternary chelates are listed for identification of the phases. XRD analysis for ternary chelates shows that the coordination of Pir alone or in the presence of Gly or PhA, to the metal ions (Fe(II), Fe(III), Co(II), Ni(II), Cu(II) and Zn(II)) change the XRD pattern of the ligands. This means that the metal ions are not fitted in the same phase of Pir, Gly or PhA. Therefore, the non-similarity of XRD pattern between the metal ions ternary chelates suggests that these chelates have a different phase structures than the Pir, Gly and PhA ligands.

In addition, on comparing the XRD spectra of the ternary chelates with the XRD spectra of the free ligands, indicate the crystallinity of the ternary chelates under study, except Fe(III)-Pir-PhA chelates, it can considered as amorphous structure.

The interdistance spacing (d, Å) and relative intensity $((I/I_0 \times 100))$ for the strongest lines characteristic for the free ligands together with their ternary chelates are indicated by bold and underline letters as shown in Tables 3 and 4; and it can be considered as a finger print for these ternary chelates.

3.6. *Structural interpretation*

The structure of the complexes was confirmed by the IR, UV-Vis, magnetic, solid reflectance, molar conductance and XRD analysis. The chelation is brought about by the pyridine nitrogen and C=O of amide groups of Pir or by the carboxylate and/or the amino groups of amino acids (Gly or PhA). The valence of the metal ions in the chelates is neutralized by displacement of carboxylate proton of amino acids. From the reflectance spectra and magnetic moment measurements, the geometrical structure of the chelates were proposed and found to be octahedral, or square planar.

As a general conclusion, Pir behaves as neutral bidentate ligands in all the chelates. While, Gly behaves as a monobasic ligand through the carboxylate group. Whereas, PhA behaves as a dibasic ligand through the carboxylate and amino groups. The structure of the chelates can be given as follows:

- Suggested structural formulae of Pir ternary chelates with Gly

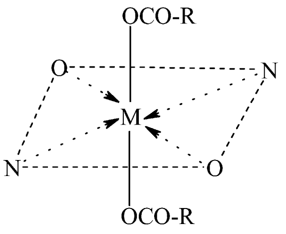

M = Fe(II), Fe(III), Co(II), Ni(II), Cu(II) and Zn(II.)
R = $-CH_2NH_2$

(Water of hydration is excluded for simplicity)

- Suggested structural formulae of Pir ternary chelates with PhA

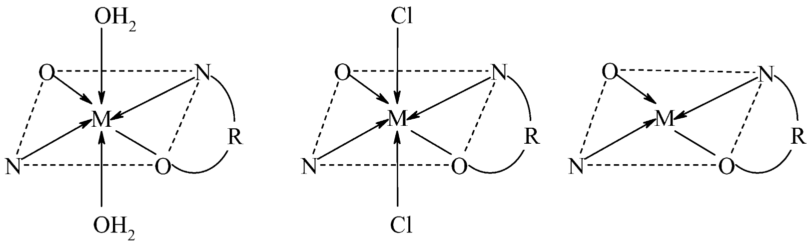

M = Fe^{II}, Co^{II} and Ni^{II}.
R = $-C_6H_5$-CH-

M = Fe^{III}.
R = $-C_6H_5$-CH-

M = Cu^{II} and Zn^{II}.
R = $-C_6H_5$-CH-

(Water of hydration is excluded for simplicity)

References

[1] D.V.R. Rao, J. Ind. Chem. Soc. 71 (1994) 533.
[2] V.V. Ramanujam, U. Krishnan, J. Ind. Chem. Soc. LVII (1980) 359.
[3] L.H. Abdel-Rahman, L.P. Battaglia, M.R. Mohamoud, Polyhedron 15 (1996) 327.
[4] H. Matsui, H. Ohtaki, Bull. Chem. Soc. Jpn. 55 (1982) 461.
[5] J. Maslowska, L. Chruscinski, Polyhedron 3 (1984) 1329.
[6] D.E. Weder, C.T. Dillon, T.W. Hambley, B.J. Kennely, P.A. Lay, J.R. Biffin, H.L. Regtop, N.M. Davies, Coord. Chem. Rev. 232 (2002) 95.
[7] J.P. Gonzalez, P.A. Todd, Drugs 34 (1987) 289.
[8] R. Cini, G. Giorgi, A. Cinquantini, C. Rossi, M. Sabat, Inorg. Chem. 29 (1990) 5197.
[9] E. Santi, M.H. Torre, E. Kremer, S.B. Etchererry, E.J. Baran, Vib. Spect. 5 (1993) 285.
[10] S. El-Khateeb, S. Abdel Fattah, S. Abdel Razeg, M. Tawakkol, Analy. Lett. 22 (1989) 101.
[11] S.K. Hadjikakou, M.A. Demertzis, J.R. Miller, D. Kolxala-Demertzis, J. Chem. Soc., Dalton Trans. (1999) 663.
[12] M.M. Abd-Elzaher, J. Chin. Chem. Soc. 48 (2001) 153.
[13] F.S. Parker, Applications of Infrared, Raman and Resonance Raman Spectroscopy in Biochemistry, Plenum Press, New York, 1983.
[14] T. Miyazawa, T. Shimanouchi, S. Mizushima, J. Chem. Phys. 29 (1958) 611.
[15] K. Nakamoto, Infrared and Raman Spectra of Inorganic and Coordination Compounds, fourth ed., Wiley, New York, 1980.
[16] D.X. West, J.K. Swearingen, J.V. Martinez, S.H. Ortega, A.K. El-Sawaf, F.V. Meurs, A. Castineiras, I. Garcia, E. Bermejo, Polyhedron 18 (1999) 2919.
[17] E.G. Ferrer, S.B. Etcheverry, E.J. Baran, Monatch. Chem. 124 (1993) 355.
[18] G.K. Sandhu, S.P. Verma, Polyhedron 6 (1987) 587.
[19] V. Aletras, N. Hadjiliadis, B. Lippert, Polyhedron 11 (1992) 1359.
[20] A.S.A. Zidan, A.I. El-Said, M.S. El-Meligy, A.A.M. Aly, O.F. Mohamed, J. Therm. Anal. 26 (2000) 665.
[21] G.G. Mohamed, N.E.A. El-Gamel, F. Teixidor, Polyhedron 20 (2001) 2689.
[22] F.H. Urena, A.L.P. Chamorro, M.N.M. Carreterro, J.M. Amigo, V. Esteve, T. Debaerdemaeker, Polyhedron 18 (1999) 2205.
[23] C.C. Su, T.Y. Tai, S.P. Wu, S.L. Wang, F.L. Liao, Polyhedron 18 (1999) 2361.
[24] A.P. Mishra, S.K. Srivastava, V. Srivastava, J. Indian Chem. Soc. 74 (1997) 487.
[25] J.A. Dean (Ed.), Lange's HandBook of Chemistry, 14th ed., New York, Mc Graw-Hill, 1992 (Table 8.35).
[26] G.G. Mohamed, N.E.A. El-Gamel, F.A.N. El-Dien, Synth. React. Inorg. Met.-Org. Chem. 31 (2001) 347.
[27] A. Hazell, C.J. Mckenzie, L.P. Nielsen, Polyhedron 19 (2000) 1333.
[28] T.J. Hubin, J.M. McCormick, S.R. Collinson, M. Buchalova, C.M. Perkins, N.W. Alcock, P.K. Kahol, A. Raghunathan, D.H. Busch, J. Am. Chem. Soc. 122 (2000) 2512.
[29] D.R. Zhu, Y. Song, Y. Xu, Y. Zhang, S.S.S. Raj, H.K. Fun, X.Z. You, Polyhedron 19 (2000) 2019.
[30] G.G. Mohamed, Z.H. Abd El-Wahab, J. Therm. Anal. 73 (2003) 347.
[31] N.K. Gaur, R. Sharma, R.S. Sindhu, J. Indian Chem. Soc. 78 (2001) 26.
[32] N. Mondal, D.K. Dey, S. Mitra, K.M. Abdul Malik, Polyhedron 19 (2000) 2707.
[33] J. Kohout, M. Hvastijova, J. Kozisek, J.G. Diaz, M. Valko, L. Jager, I. Svoboda, Inorg. Chim. Acta. 287 (1999) 186.
[34] N.R.S. Kumar, M. Nethiji, K.C. Patil, Polyhedron 10 (1991) 365.
[35] M.F. Iskander, T.E. Khalil, R. Werner, W. Haase, I. Svoboda, H. Fuess, Polyhedron 19 (2000) 949.
[36] J. Manonmani, R. Thirumurugan, M. Kandaswamy, M. Kuppayee, S.S.S. Raj, M.N. Ponnuswamy, G. Shanmugam, H.K. Fun, Polyhedron 19 (2000) 2011.
[37] J. Sanmartin, M.R. Bermejo, A.M.G. Deibe, M. Maneiro, C. Lage, A.J.C. Filho, Polyhedron 19 (2000) 185.
[38] V.P. Krzyminiewska, H. Litkowska, W.R. Paryzek, Monatshefte Fur Chemie 130 (1999) 243.
[39] K. Bertoncello, G.D. Fallon, K.S. Murray, E.R.T. Tiekink, Inorg. Chem. 30 (1991) 3562.
[40] Natl. Bur. Stand (U.S.) Monogr. 25 (1980) 1734.
[41] Khawas, Acta Crystallogr., Sect. B 27B (1971) 1517.